IS-PORTO 2023 PROCEEDINGS

Proceedings of the 8th International Symposium on DEFORMATION CHARACTERISTICS OF GEOMATERIALS Porto, 3rd - 6th September 2023

Transient phase in shear zone formation in sands

Sudhanshu Rathore[1], *Abhijit* Hegde[1], and *Tejas Gorur* Murthy[1#]

[1]*Indian Institute of Science, Department of Civil Engineering, Bangalore, India*
[#]*Corresponding author: tejas@iisc.ac.in*

ABSTRACT

An experimental study has been made to study the emergence of narrow shear zones ("shear bands"), in uniformly graded quartzitic sand under dry conditions using the model setup of orthogonal cutting. A fixed region of interest around the stationary tool is imaged using a high-resolution and high-speed camera and further analyzed using Particle Image Velocimetry (PIV) algorithm to obtain the flow (velocity) fields. The velocity field maps of the near tool tip region demonstrate sharp change in the motion of sand particles along with the formation of a "dead zone" – a region of material stagnation or no flow. This extent of the dead zone was found to fluctuate in time for a given cutting speed, and no significant effect of the cutting speed (or strain rate) is observed in the propagation of dead zone size. The dynamic repose angle of the evolving sand pile in front of the tool increases initially and then attains a steady value of around 40°. The regions of intense straining in the sands were revealed in the effective strain rate fields. The shear localization was seen to emerge from the tooltip and propagate toward the free surface. The inclination angle of these bands evolves periodically with time and showed a decreasing trend due to an increase in the surcharge. The oscillatory force signatures suggested that every undisturbed ensemble of sands, on reaching the tool vicinity, undergoes material softening (dilation) followed by hardening(compaction), which is also reflected in the periodic formation and destruction of shear bands.

Keywords: Orthogonal cutting; shear bands; oscillatory behavior.

1. Introduction and Background

The mechanism of cutting is at the core of several civil engineering operations such as ploughing in farmlands, trenching, excavation at construction sites, underwater trenching for offshore pipeline burial, quarrying for aggregates, dredging for removal of seabed deposits, tunnel boring, and natural phenomena such as landslides, avalanches, burrowing, etc. These problems are close to plane strain conditions, with the failure driven by the creation of localized and intense shearing. Ploughing or soil cutting is an operation in which geomaterials, like soils and rocks, are cut and displaced under a range of depths and speeds. Soil undergoes large progressive, irrecoverable deformation during cutting. The interaction of the cutting tool with the soil causes large plastic deformations in the soil. This soil-tool interaction depends on soil characteristics, machine/tool parameters, and soil-tool interface properties (Payne 1956; Payne and Tanner 1959; Luth and Wismer 1971). The underlying kinematics of particle displacements and resistive forces observed during cutting in soils are crucial and need to be quantified for efficient tool design for earth-moving operations. The simple yet significant experimental model to study the deformation characteristics and failure mechanisms in soil cutting is the orthogonal cutting model.

Formation of shear bands in soils is commonplace in conventional geotechnical tests like the triaxial compression test, unconfined compression test, biaxial compression test, etc. Though shear band properties have been studied using these elemental tests, their occurrence both spatially and temporally is not controlled. On the other hand, the orthogonal cutting setup allows control of the occurrence of shear bands in a specific location providing an opportunity for detailed characterization.

There have been abundant studies on soil cutting (both in 2D and 3D) for the measurement and prediction of tool (or cutting) forces and loads but studies focusing on the deformation features are few and far between. Selig & Nelson (1964) qualitatively studied the pattern of deformations during orthogonal cutting in medium-dense dry Ottawa sands and other soils. They used grids of colored particles to visualize the planar deformations. Gravish et. al (2010,2014) observed the effects of initial packing density on the force and flow dynamics of plowed granular material and modeled the cutting force as a function of kinetic friction and shear band inclination. Kobayakawa et al. (2018) conducted large-scale discrete element modeling and numerically validated the results of experiments.

In this work, the transient state of cutting and its evolution to a steady state of cutting is presented. An image-based technique was used to measure the deformation fields. The initiation and propagation of shear bands have been investigated, and comparisons between theoretical predictions and experimental results are made for the cutting forces.

2. Experiments

A series of in-plane orthogonal cutting experiments were carried out using a lab-scale setup shown in Fig. 1. A box made of high-strength Aluminium (with inner dimensions of 55.5 *16 * 1.5 cm) was used to contain the model granular geo material (quarried) quartz sands.

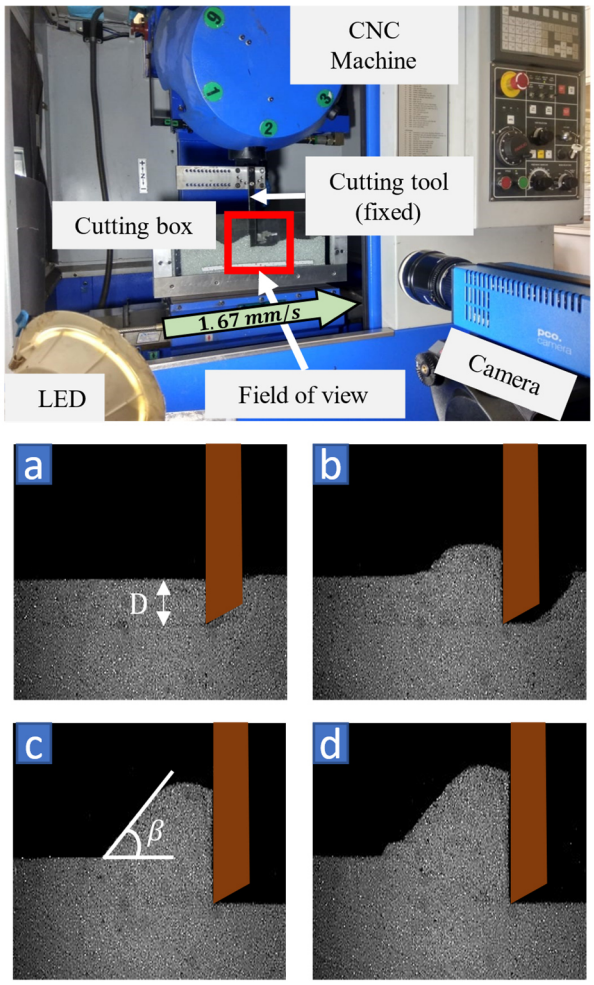

Figure 1. Orthogonal cutting set-up on a CNC machine: High-speed, high-resolution imaging was done, and a fixed field of view captured during the cutting is highlighted (red square). Four sample images (a-b-c-d) of cutting with a vertical (rake angle = 0°) tool at an initial depth (D) of 20mm and cutting speed of 1.67 mm/s are shown.

The top surface of the box was kept open to fill in the sands using the air pluviation technique, and the front face was made of glass to visualize the displacement of particles. The dry density of filled-in sands was kept constant at 1.5 g/cc for all the tests. The particle size gradation of the model sand is presented in Fig. 2. The mean grain size was 0.45mm and, Cu and Cc values were 3.09 and 1.18, respectively, classified as poorly graded sand (SP).

The cutting box was fixed on a CNC machine (AMS Spark-XL). A vertical flat-faced cutting tool was fitted to the spindle of the machine and lowered carefully into the box to the required depth. The cutting tool was made of high-speed steel and had a width of 1.5 cm to fit the box's width to maintain plane strain conditions. With the tool kept stationary, the cutting box was moved unidirectionally at a constant predefined speed of cut. A high-speed, high-resolution camera (pco 1200hs) was used to image the cutting process. The glass front of the box was uniformly illuminated using an LED light source. The image capturing rate was estimated for different cutting speeds such that a constant movement of 3 pixels was maintained between consecutive frames for all experiments with different speeds of cut. The spatial resolution of this optical setup was around 193 µm (magnification of 5.2 pixels/mm) and kept unchanged throughout the series of tests. The size of the images was 1024*1240 pixels. The field of view, fixed with respect to the tool, is shown in Fig. 1.

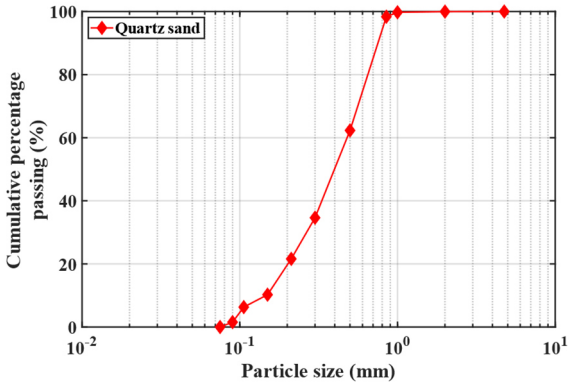

Figure 2. Particle size gradation of sands used in experiments.

The captured images were analyzed using a PIV code in MATLAB to obtain the incremental 2-dimensional displacements or the velocity fields. PIV is a digital image correlation-based technique used to estimate the velocity of the deforming material (Hegde and Murthy 2022).

3. Results and Discussion

The results of orthogonal cutting experiments at zero rake angle and initial depth (D) of 20 mm with imposed cutting speed (v_c) of 1.67 mm/s are presented here. The magnitude of the computed velocity field and strain rate field have been normalized by the imposed speed, v_c, and strain rate factor - v_c /D, respectively. The horizontal and vertical dimensions of the box were normalized with respect to initial cutting depth as X/D and Y/D, respectively. The tool displacement (u), measured from the frame of reference attached to the cutting box, was normalized by initial cutting depth as u/D.

3.1. Dynamic repose and transient stage

Sand undergoes severe plastic deformation during cutting. This deformation is a function of the rake angle, depth of cut, and particle characteristics (Hegde 2022). Fig. 3 shows the typical evolution of sand pile inclination (β) as a function of tool displacement. The repose angle increases initially and then reaches a steady value of around 40° at a drag distance of 1-1.5D - indicating that the displaced material has attained a steady shape. The repose angle remained unchanged for the cutting experiments with different speeds, spanning 3 orders of magnitude (0.1667 - 166.67 mm/s). The transient stage of cutting exists till the dynamic pile inclination reaches a steady value, and therefore, the tool distance of 0-1D is considered the transient stage of cutting in these experiments.

The steady-state repose value of 40° was found to be close to the average friction angle value at the critical state during hollow cylinder tests (Kandasami and Murthy 2017) for intermediate stress ratio ('b' parameter) of 0.2-0.4 (plane strain conditions).

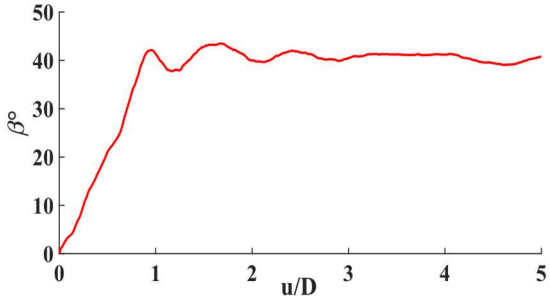

Figure 3. Evolution of sand-pile inclination ahead of the tool rake face.

3.2. Velocity, strain rate, and dead zone fields

The PIV analysis on the successive images captured during the cutting yields incremental horizontal (v_x) and vertical (v_y) displacements. Fig. 5a presents the resultant velocity vector fields at different instances of cutting during the transient phase. These stages of cutting are marked at the normalized tool displacements, u/D, of – 0, 0.25, 0.5, 0.75, 2.5, and 1. The material below the tooltip is seen to be unaffected during cutting as the velocity remains unchanged in this region. Velocity bifurcations are observed in the region above and near the tooltip, wherein the sand particles experience a sharp change in the direction and magnitude of their motion. All the sand particles were moved horizontally within the box with the tool inserted. As the material approaches the tool, the sand particles begin to climb upwards on the tool rake face, creating a non-zero vertical velocity. There is also a gradual reduction in the resultant velocity magnitude with further tool movement. Ultimately, the horizontal velocity component of the sand pile becomes insignificant, and the material, in general, moves upward along the tool face. The direction of vector displacements, obtained from PIV, allowed visualization of a wedge of the sand pile in front of the tool that moves upwards, largely, relative to the tool. There is also a region of, approximately, zero resultant velocity ("dead zone") at the tooltip. These dead zones occur in experiments carried out at different speeds of cut. In this study, the dead zones vary with shape and size as the cutting advances in sands, however, there is no effect of these dead zones as such on the general failure behavior of sands during cutting.

Strain rate was also evaluated in all the experiments. The strain rate indicates a spatial jump in the velocity, or a region of intense deformation over time elapse. The planar (2-dimensional) strain rate tensor was obtained by computing the spatial differentiation of the in-plane velocity vector field. The elements of this tensor were further used to compute the effective strain rate through Eq.(1).

$$\dot{\epsilon}_{eff} = \frac{2}{3}\sqrt{\frac{1}{2}\left[\left(\dot{\epsilon}_{xx} - \dot{\epsilon}_{yy}\right)^2 + \dot{\epsilon}_{xx}^2 + \dot{\epsilon}_{yy}^2 + \frac{3}{2}\dot{\epsilon}_{xy}^2\right]} \quad (1)$$

where,

$\dot{\epsilon}_{xx} = \partial v_x/\partial x$ being the component of strain rate tensor along the direction of cutting (x-axis)

$\dot{\epsilon}_{yy} = \partial v_y/\partial y$ being the component of strain rate tensor normal to the direction of cutting (y-axis)

$\dot{\epsilon}_{xy} = 0.5(\partial v_x/\partial y + \partial v_y/\partial x)$ being the shear component of strain rate tensor

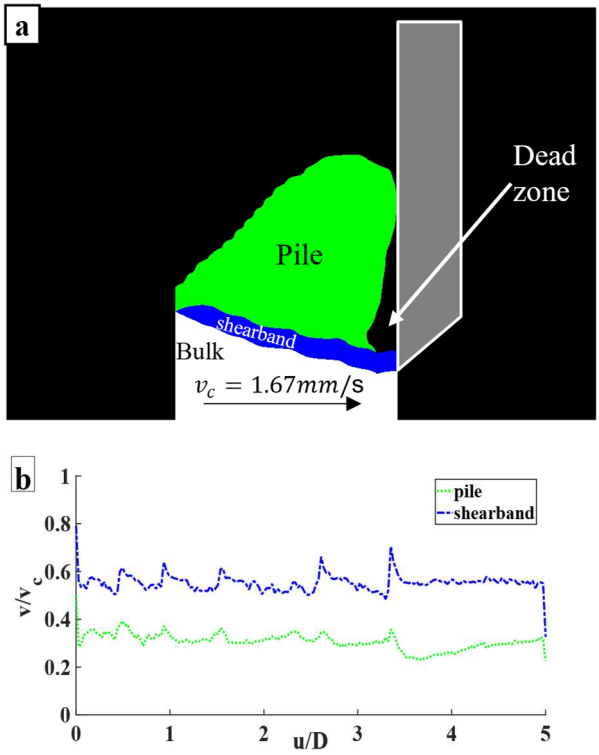

Figure 4. (a) A masked image showing different zones- pile, shear band, dead zone, and bulk- in the sands appearing during cutting. (b) Variation of mean velocities in the shear band and the pile of sand above it.

Effective strain rate contours during the transient cutting phase are shown in Fig. 5b. At the initiation of cutting, the instantaneous strains near the tool are diffused over a small region in the sands. It was observed to take around 10 frames (tool displacement of ~5.5mm) for the strain to localize in a narrow region and reach the free surface from the tooltip. These localized strains are termed shear bands which result from flow bifurcations (velocity jumps) during cutting. The magnitude of the strain rate in the shear band region is 2 times the imposed strain rates, irrespective of cutting speed. Other noticeable regions of high strain rates, less intense than shear bands, are found to appear at the tool-sand interface and the free surface of the pile.

Further, variation of velocity magnitudes in the shear band and in the accumulated chip (henceforth referred to as sand pile) ahead of the tool rake are also presented as a function of time. The image analysis of strain rate fields and velocity fields allow demarcation of the shear band and pile as shown in Fig. 4a. A combination of adaptive and global thresholding on these images was used to demarcate the shear band.

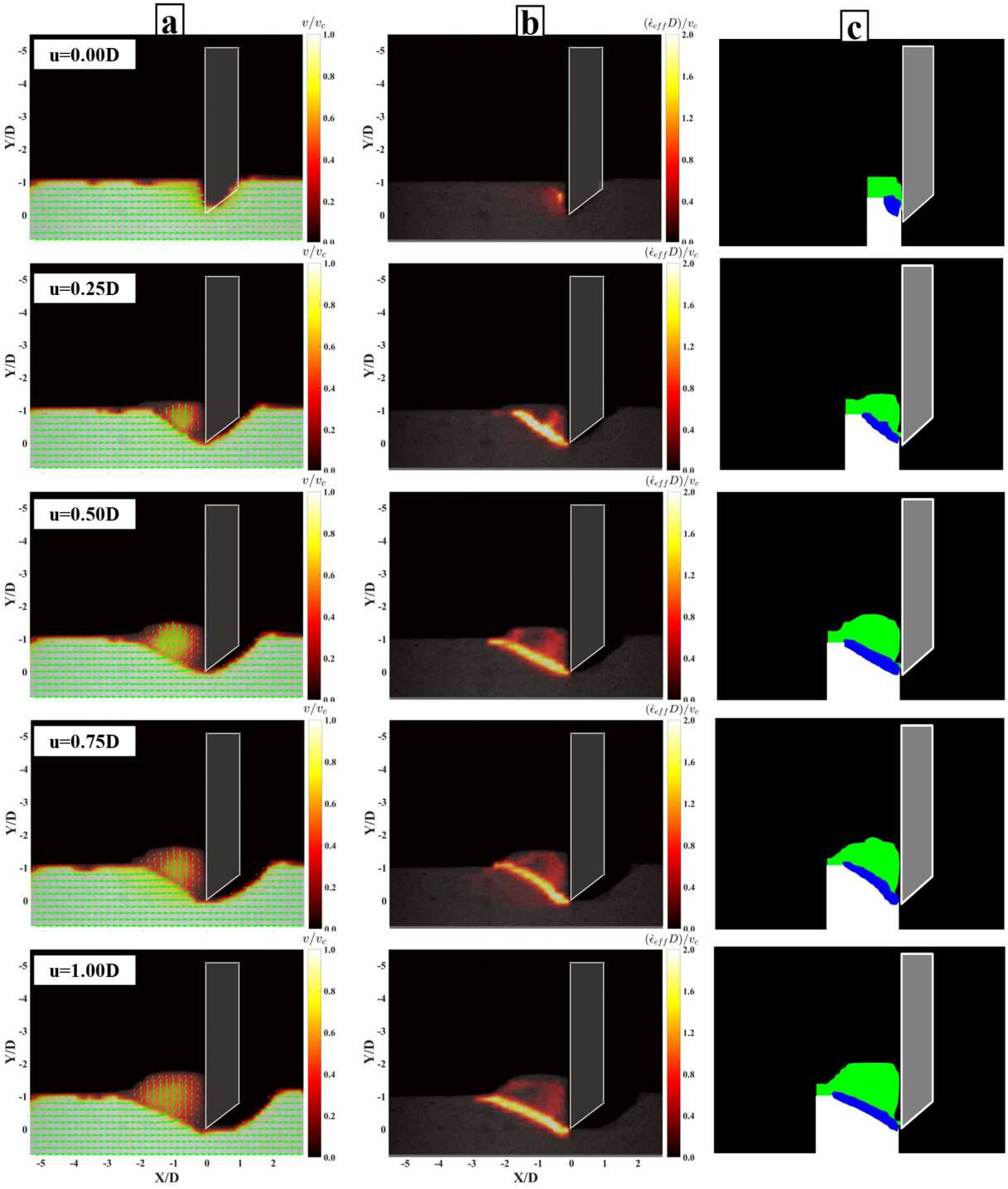

Figure 5. (a) Velocity field corresponding to 5 equally spaced time instances (1st column, top to bottom) when the tool has traversed 0D,0.25D,0.5D,0.75D, and 1D. (b) Strain rate field corresponding to velocity field maps in (a). (c) Respective mask images showing the variation of dead zone (black) trapped between pile (green), shear band (blue), and the tool rake face. The dead zone shape and size vary in time.

Fig. 4b shows that the magnitude of the flow velocity in the shear bands was found to be around 80% of the imposed cutting speed at the initiation of cutting and then fluctuated around 55% during the steady state of cutting. The velocity magnitude in the pile at the initiation was 60% and fluctuated around 30%, indicating that retardation is more dominant in the pile than in the shear band. Also, the unaffected zone below the shear band is at 100% of imposed velocity. Velocity bifurcations or regions of different velocities emerge as the cutting occurs. The spikes in both graphs correspond to the switch of the shear band from one in active mode to another in insipient inactive mode (Gravish et al. 2010).

3.3. Shear band characterization and behavior

Fig. 6a presents the typical geometrical parameters of the shear band observed in the experiments. The extent of the localization is quantified by estimating the shear band length(L) and width(W), while the orientation of the localization is measured through the shear band inclination angle (θ). These shear band parameters are extracted from strain rate field maps using the Standard Hough Transform (SHT) – a technique to identify known geometries like lines, circles, etc., using their respective parametric equations. For the case of straight lines, SHT implementation yields the end coordinates of the identified straight line and its inclination angle (Duda and Hart 1972; Hegde and Murthy 2022).

Fig. 6b shows a general propagation of shear band thickness with the tool displacement. The mean thickness of the shear band was about 10 times the particle size (d_p). The peaks in the thickness appear at time instances when more than one shear band is present, i.e. when one of the shear bands diffuses, another region of localization emerges. This is also observed when the inclination angles are measured (in Fig. 6c), wherein the peaks correspond to the instance of the shear band switching from one in active mode to another in incipient mode.

The mean shear band angle decreases due to the increase in the surcharge. The shear band length continually increases as seen in Fig. 6d. The shear band remains mostly pinned between the tooltip and the tip of the sand pile at the initial horizontal surface. This base of the pile moves farther due to the increasing size of the pile, also increasing the shear band length.

3.4. Cutting forces – experimental and model

The cutting tool pushes through the sand continuously and thus experiences reaction forces on its rake face. The major components of the tool forces are – horizontal draft (normal to the rake) and vertical lift (parallel to the rake and acting downwards). These force components were measured experimentally by attaching a force transducer to the rake face of the tool, and the resultant cutting force was calculated. An analytical estimate of the resultant force (F_{tool}) was also carried out based on the limit equilibrium approach modified with the inclusion of inertial forces (F^a). This analytical model was proposed by (Swick and Perumpral 1988) to study the soil-tool interaction under dynamic conditions.

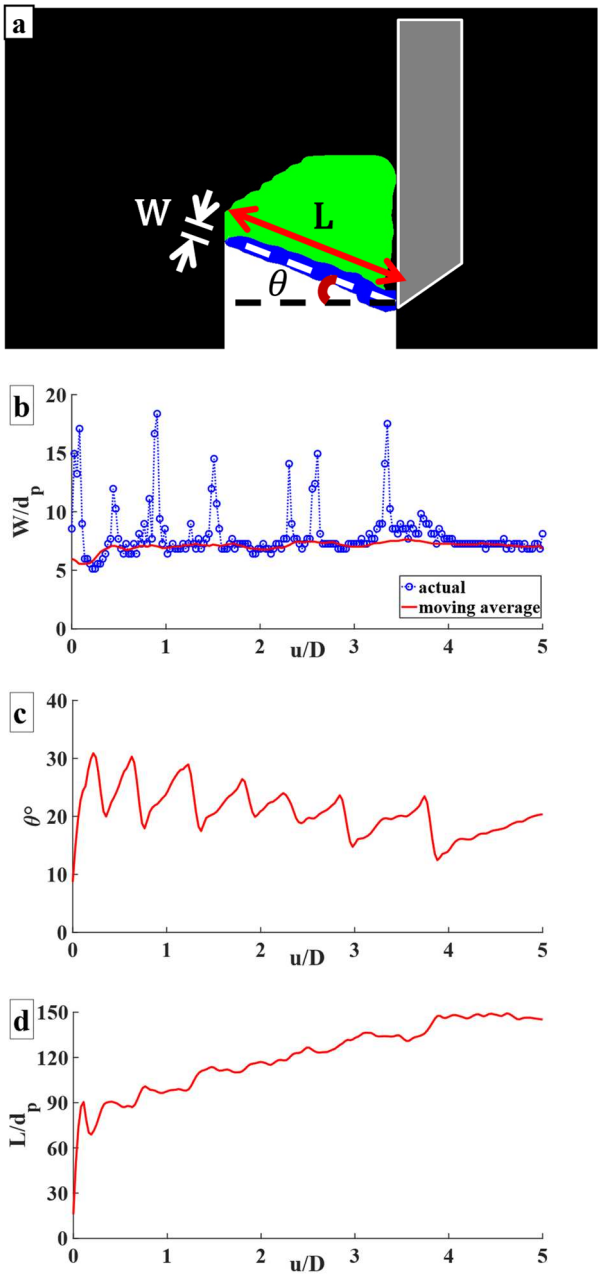

Figure 6. (a) Masked image showing geometric parameters of the shear band – length (L), width (W), and inclination (θ). Evolution of (b) normalized width(W/d_p), (c) normalized length (L/d_p), and (d) angle (θ) of the shear band with normalized tool displacement.

The model forces were estimated using Eq. (2) and (3) below:

$$F^a = \frac{\gamma B D v^2}{g cos\theta} \tag{2}$$

$$F_{tool} = \frac{W sin(\theta+\beta)+F^a cos\beta}{cos(\theta+\delta+\beta)} \tag{3}$$

where:

B = Tool width, 15mm; γ = Bulk unit weight of pile, 14.715 kN/m^3; v = Speed of cut, 1.67mm/s; δ = soil-tool interface friction angle, 10°, β = Critical friction

angle under plane strain, 40°, W = Weight of mobilized sand pile in N.

The experimental and model estimates of the forces are shown in Fig. 7. The behavior of a typical force signature is oscillatory with an effective increase in the mean forces.

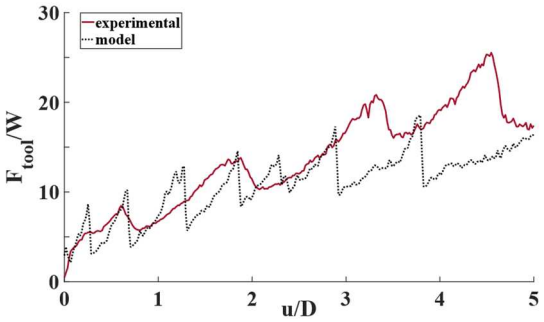

Figure 7. A typical signature of resultant (normalized) cutting force during 2-d orthogonal cutting.

After the formation of the initial shear band, the sands in the wedge above it are being pushed (compacted), thus causing an increase in the forces. Following some tool displacement, a new failure plane in the undisturbed ensemble of sands forms, and thus force drops momentarily. This material softening (dilation) behavior is followed by hardening(compaction) which is also reflected in the periodic creation and destruction of shear bands.

Shear bands are formed continuously through this process. The periodicity observed in the measured forces can be attributed to the cycles of dilation and compaction which is clearly observed in the effective shear rate fields. Gravish et al. (2010) and Selig & Nelson (1964) found similar behavior, additionally, Gravish et al. (2010) observed that the cutting forces increase linearly with the packing density and periodic signatures in the cutting forces exist for the denser ensemble. The lateral confinement that has been put to create the plane strain deformations cause the pile height, and hence the effective depth of cut to increase with the progression of cutting. This also leads to the effective increase of mean forces as the amount of sand to be displaced in each successive stage increases. The experimental force measurements for cutting sands with different speeds were found to match well with the model (Fig. 7).

4. Conclusions

Orthogonal cutting experiments were performed in dry sands, and the deformation characteristics were studied using image analysis. The transient phase of cutting was defined based on the repose behavior of the accumulated pile, whose size and shape evolve in time. The dynamic repose angle was observed to attain a value close to 40° after a tool displacement of 1D, and this value is found to be close to the critical state friction angle under plane strain conditions. In the velocity contour fields, flow bifurcation is observed at the tooltip vicinity. These bifurcations or velocity jumps are also the regions of high strain rates or shear bands. These regions are diffused at the beginning of the cutting but eventually form a narrow band-“ shear band”. The extent and orientation of these strain localization regions are studied through the evolution of the length, width, and inclination angle of shear bands. The shear band angle showed a decreasing trend with oscillatory behavior while the shear band length effectively increased. Further, the cutting forces are also found to increase, with periodic fluctuations, as the cutting progresses. The oscillatory behavior of shear band angle and cutting forces are due to the periodic creation and destruction of shear bands, which is visually observed in the effective strain rate maps.

References

Duda, R. O. and P. E. Hart. 1972. “Use of the Hough transformation to detect lines and curves in pictures”. Communications of the ACM 15.1, pp. 11–15. https://doi.org/10.1145/361237.361242

Gravish, N., P. B. Umbanhowar, and D. I. Goldman. 2010. "Force and flow transition in plowed granular media." Physical review letters 105, no. 12: 128301.https://doi.org/10.1103/PhysRevLett.105.128301

Gravish, N., P. B. Umbanhowar, and D. I. Goldman. 2014. "Force and flow at the onset of drag in plowed granular media." Physical Review E 89, no. 4: 042202.https://doi.org/10.1103/PhysRevE.89.042202

Hegde, A. 2022. “Mechanics of cutting in granular media” PhD diss., Indian Institute of Science, https://etd.iisc.ac.in/handle/2005/5828

Hegde, A., and T. G. Murthy. 2022. "Experimental studies on deformation of granular materials during orthogonal cutting." Granular Matter 24, no. 3: 1-22.https://doi.org/10.1007/s10035-022-01227-5

Kandasami, R. K., and T. G. Murthy. 2017. "Manifestation of particle morphology on the mechanical behaviour of granular ensembles." Granular Matter 19, no. 2: 1-13. https://doi.org/10.1007/s10035-017-0703-z

Kobayakawa, M., S. Miyai, T. Tsuji, and T. Tanaka. 2018. "Local dilation and compaction of granular materials induced by plate drag." Physical Review E 98, no. 5: 052907.https://doi.org/10.1103/PhysRevE.98.052907

Murthy, T. G., C. Huang, and S. Chandrasekar. 2008. "Characterization of deformation field in plane-strain indentation of metals." J Physics D: Applied Physics 41, no. 7: 074026.https://doi.org/10.1088/0022-3727/41/7/074026

Payne, P. C. J. 1956. “The relationship between the mechanical properties of soil and the performance of simple cultivation implements”. J Agricultural Engineering Research 1.1, pp. 23–50.

Payne, P. C. J. and D. W. Tanner. 1959. “The relationship between rake angle and the performance of simple cultivation implements”. J Agricultural Engineering Research 4.4, pp. 312–325

Selig, E.T. and Nelson, R.D. 1964. “Observations of soil cutting with blades.” J Terramechanics, 1(3), pp.32-53. https://doi.org/10.1016/0022-4898(64)90038-2

Swick, W. C., & Perumpral, J. V. 1988. “A model for predicting soil-tool interaction.” J Terramechanics, 25(1). 43-56. https://doi.org/10.1016/0022-4898(88)90061-4

White, D. J., W. A. Take, and M. D. Bolton. 2003. "Soil deformation measurement using particle image velocimetry (PIV) and photogrammetry." Geotechnique 53, no. 7: 619-631..https://doi.org/10.1680/geot.2003.53.7.619

Wismer, R. D., and H. J. Luth. 1971. “Rate effects in soil cutting.” No. 710179. SAE Technical Paper. https://doi.org/10.4271/710179